FITTING PROCEDURE FOR PV PANEL MEASURED CURRENT-VOLTAGE CHARACTERISTICS

Heidi Kalliojärvi-Viljakainen, Kari Lappalainen, Seppo Valkealahti
Tampere University, Electrical Engineering, Tampere, Finland
E-mail: heidi.kalliojarvi-viljakainen@tuni.fi, kari.lappalainen@tuni.fi, seppo.valkealahti@tuni.fi

ABSTRACT: Current-voltage curve measurements are a potential tool for efficient monitoring and diagnosis of photovoltaic (PV) panels and systems. To determine indicators of aging, degradation and other such phenomena of PV panels, an attractive option is to fit an electrical model of the PV panels to measured data in order to detect changes. However, raw measurement data usually contains measurement noise and other factors that can distort the analysis. The fitting process is challenging for instance, by the fact that the measurement points are unevenly distributed on the current-voltage curve, being mainly clustered on the open-circuit region. This unintentional weight can distort the fit. To address these issues, the present paper introduces a procedure for fitting an electrical model of the PV panels to the measured current-voltage curves so as to alleviate the above problems. The proposed approach is a prerequisite for a reliable diagnosis of the PV system status.
Keywords: PV panel, single-diode model, *I-U* curve, fitting

1 INTRODUCTION

For the evaluation of the photovoltaic (PV) panel condition, the single-diode model parameters estimated from the measured PV panel current-voltage (*I-U*) characteristic curves can serve as a valuable tool. Conventionally, the parameters are extracted from the standard test condition (STC) values for current and voltage reported in the PV panel datasheet and then translated to actual outdoor conditions to simulate the operation of PV systems. Using this approach directly on the measured curves would, however, make the information dependent on external factors and, thereby, make the reliable comparison of different parameter sets challenging when obtained under different measurement conditions. To address this issue, an inverse approach must be adopted, involving also the conversion of parameters extracted from a measured *I-U* curve to STC. To this end, the authors of [1] investigated the reverse conversion of parameter translation formulae initially introduced in [2]. For successful comparison of different *I-U* curves, reliable estimation of the parameters is mandatory.

Accurate determination of single-diode model parameters is difficult due to measurement noise and other deficiencies occurring in the raw *I-U* measurement data. In this light, it is important to take the specific properties of the *I-U* data inflicted by the used measurement device into account. All the raw data produced by commonly used *I-U* curve tracers suffers from certain disadvantages. For instance, the measurement points are spaced evenly in terms of time and, therefore, tend to cluster towards the ends of the *I-U* curve. The problem appears particularly in the vicinity of the open-circuit point, which comprises a vast majority of the measured points, while the measurement points are more sparsely located in the short-circuit region. The phenomenon has been explained in more detail in [3]. The clustering of the points results in an undesired high weight of the open-circuit region in the fitting process; the authors of [4] observed that certain data point distributions make the usual fitting based on root-mean-square error (RMSE) unreliable. The problem of uneven weighting between the points has been emphasized in [5] as well. To improve the fit quality, the authors of [6] sampled the PV cell current into equidistant voltage values. However, it has been stated in [5] that then approaches such as the least squares fit provide an excellent fit to the open-circuit region at the expense of the fit quality to the short-circuit region. In [7], the quality problems of the fit have been discussed and the weighted least squares fit has been applied to the double-diode model to obtain more reliable parameter values. The authors of [8] introduced a double sweep *I-U* curve tracing technique to mitigate the uneven distance problem. However, their design is still a prototype and most existing *I-U* curve tracers are subject to disadvantages described above. The issue of noisy and unequally weighted measurement data is addressed in [9], which introduces a preprocessing procedure for *I-U* measurement data.

As a continuation for the work in [9], this paper presents various approaches for the pretreatment of measurement points to achieve a more accurate fit of the electrical model to the measurements of the *I-U* curves. The fitting of the single-diode model equation has been performed by applying the MATLAB function fit.m. The emphasis is on ensuring the functionality of the pretreatment approaches such that fitted *I-U* curves are reliable sources for estimating single-diode model parameters and external operating conditions. Further, conversion of parameters to STC must be on a stable footing so that the results can be reliably compared over the life span of PV panels.

The paper is organized as follows. Section 2 is devoted for describing the used approaches as well as the used empirical data. Section 3 presents the proposed procedure. Section 4 reports the results and provides discussion about them. Finally, Section 5 closes the paper.

2 METHODS AND DATA

2.1 The single-diode model

The operation of a PV panel is modelled using the single-diode model. It provides the following implicit equation for the operational DC current I and voltage U

$$I = I_{\mathrm{ph}} - I_{\mathrm{o}}\left(e^{\frac{U+IR_{\mathrm{s}}}{AU_{\mathrm{t}}}} - 1\right) - \frac{U+IR_{\mathrm{s}}}{R_{\mathrm{h}}}, \quad (1)$$

where I_{ph} is the photogenerated current, I_{o} the diode saturation current, A the diode ideality factor, R_{s} the series resistance and R_{h} the shunt resistance. $U_{\mathrm{t}} = N_{\mathrm{s}}kT/q$ is the thermal voltage, where N_{s} is the number of series-connected cells in the panel, T the panel temperature, k the Boltzmann constant and q the elementary charge. The

single-diode model is described in detail in [10], for instance.

2.2 The used empirical data

The used measurement data has been gathered from the solar PV power research plant installed on the rooftop of Tampere University, Tampere, Finland [11]. The plant consists of 69 multi-crystalline silicon NAPS NP190GKg panels. The used data comprises single-panel seven-hour *I-U* curve tracer measurements at a sampling frequency of 1 Hz utilizing the electronic load method with IGBTs, as well as measurements of the outdoor conditions. The measured *I-U* curves consist of 4000 measurement points each, with the measurement sweep direction being from open-circuit to short-circuit. Irradiance (G) and PV panel backplate temperature were measured via SPLite2 and Pt100 sensors, respectively.

2.3 The preliminary preprocessing procedure

At first, a preprocessing procedure introduced in [9] is applied to the raw *I-U* curve measurement data in order to remove abnormal measurement points, i.e., clear anomalies from the trend of the *I-U* curve. The *I-U* curve is divided into small overlapping intervals whose lengths are certain fractions of the maximum power point (MPP) voltage. Then, every interval is approximated by a linear fit and the interquartile range (IQR) of the distance of the points from the fitted line is calculated. If the distance related to a point exceeds the limit 1.5IQR, the point is discarded as an outlier.

3 THE INVESTIGATED APPROACHES

After the preliminary outlier elimination step, four different approaches were applied to find the best way to select measurement points for curve fitting. These approaches were analyzed based on the accuracy and performance of the single-diode model fitted to the selected points.

3.1 Reference approach

The reference approach is to make the fit into the preprocessed data without any point selection approach.

3.2 Representative points approach

This approach is the final part of the procedure presented in [9]. The detected MPP divides the *I-U* curve into constant current and constant voltage regions. Both regions are divided into an equal number of small equidistant intervals so that the current side is evenly spaced in terms of voltage and the voltage side is evenly spaced in terms of current. The averaged current and voltage values of each interval form the representative points to be used in the fitting process.

3.3 Nine points approach

This approach mimics the conventional fitting of an *I-U* curve to the three quantitative points. However, the used single-diode model fitting procedure requires at least five data points for fitting, as it produces five output quantity values (see Section 3.5). To ensure that the curvature around the MPP is captured, nine points are selected for fitting such that three points are chosen from each quantitative region. The three points at each end of the curve are chosen close to each other by averaging appropriate sequences of points in order to form a point-like combination. This condition is simple to satisfy in the heavily weighted open-circuit end of the curve, where the points are densely located. In contrast, the sparse location of the measurement points in the short-circuit end makes it challenging to determine the three representative points from the very end of the *I-U* curve without letting the noise to distort the approximation of the correct short-circuit current level. The flat region of the current measurement sweep provided by the *I-U* curve tracer comprises the most part of the constant current region jointly with the noisy end of the *I-U* curve. It is observed that the higher the irradiance is, the shorter is the flat part of the current measurement sweep. Regardless of the irradiance level, it is experimentally found that this part contains hundreds of points and at least the last 150 points of the measured *I-U* curve are accumulated in the end of the curve. This also serves as the experimental criteria to be used in this study; 150 points from the both ends of the curve are selected and the arithmetic means of the voltage and current of the three consecutive sets of 50 points are calculated. Thus, the representative points are located sufficiently close to each other at both ends of the *I-U* curve. The same criterion is applied to MPP region, where 150 neighboring points spread around the MPP, detected as in [9], are divided into three sets, each of which is then subjected to the above-mentioned averaging of voltage and current. Thus, the fitted curve is not forced through the MPP; such a choice is performed in preference of the capability of the fit to capture the curvature. The equal weighting of the selected nine points is obvious.

3.4 Three regions approach

This approach resembles the previous one, with the main difference being that it exploits the exact shape of the measured *I-U* curve at and around the MPP; three equally long sequences of measurement points are selected from each quantitative regions of the *I-U* curve. In the MPP region 90 % of the detected MPP power is used as a limit for selecting measurement points. However, the number of measurement points on this region depends on each *I-U* curve. In order to maintain the same weighting in all the regions, an equal number of points are selected from the short-circuit and open voltage regions of the *I-U* curve as from the MPP region.

3.5 The fitting procedure

The used single-diode model fitting procedure, utilizing the fit.m function in MATLAB, has been earlier exploited and described in more detail in [9]. It takes the measured PV current and voltage values as its inputs and provides the five-tuple (I_{ph}, I_o, R_s, R_h, T) as its output. The constant value of A = 1.3 for multi-crystalline silicon is adopted from [12]. The fitting procedure also enables the calculation of irradiance via the formula

$$I_{SC} = \frac{G}{G_{STC}} I_{SC,\,STC}(1 + K_I(T - T_{STC})), \qquad (2)$$

where $I_{SC,\,STC}$ is the short-circuit current in STC and K_I the temperature coefficient of the short-circuit current reported in the PV panel datasheet.

4 RESULTS AND DISCUSSION

The selection of data points for the reference approach is obvious and the representative points approach has

already been visualized in [9]. Fig. 1 illustrates the selection of points for the nine points and three regions approaches, marked by green and red colors, respectively. Fig. 2 reveals that due to the accumulation of points in the open-circuit voltage region, the set of points selected by the three regions approach resemble a point rather than a part of a line.

In order to evaluate the effect of the four different preprocessing approaches of the measured *I-U* curves for the actual fitting process of the single-diode model, Fig. 3 and Table I show the RMSE values resulting from fitting the single-diode model for a two-hour measurement data. All the approaches show sharp peaks in RMSE around 2400 seconds due to temporary partial shading. The highest median RMSE appears for the nine points approach, resulting from the fact that the fit need not pass through the detected MPP. However, the interquartile range of the RMSE provided by the nine points approach is the second lowest, indicating that the fit quality varies little. The second highest RMSE median value is provided by the three regions approach. Despite of that this approach produces the smallest IQR showing that the fit quality remains most homogeneous for this approach. The second smallest RMSE median value appears for the reference approach, but the largest IQR reveals that the fit quality varies most. A possible explanation might lie in the large variation of the identified model parameters at low irradiance levels, which becomes visible in the later discussion regarding the series resistance. The smallest median and the third smallest IQR of the RMSE are for the representative point approach, confirming both the accuracy and the stability of the fit. In overall, the representative point approach appears to be the best in terms of RMSE, but also the three regions and nine points approaches indicate development potential.

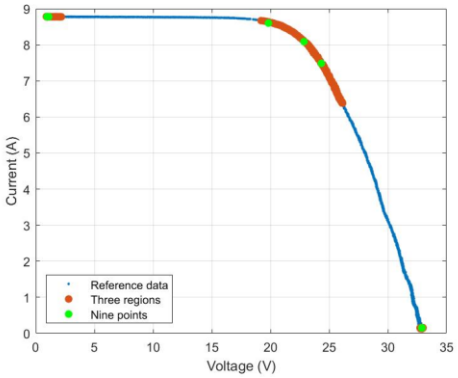

Figure 1: Selection of data points for the three regions and nine points approaches on a preprocessed *I-U* curve measured at a high irradiance level.

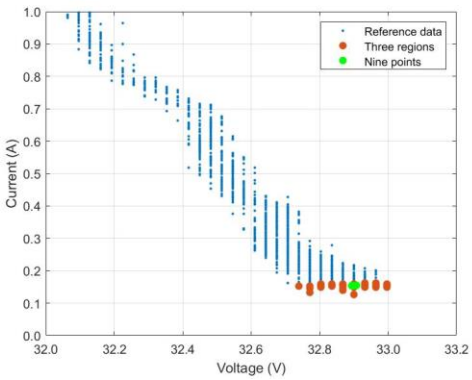

Figure 2: A snapshot of the open-circuit end of the *I-U* curve in Fig. 1.

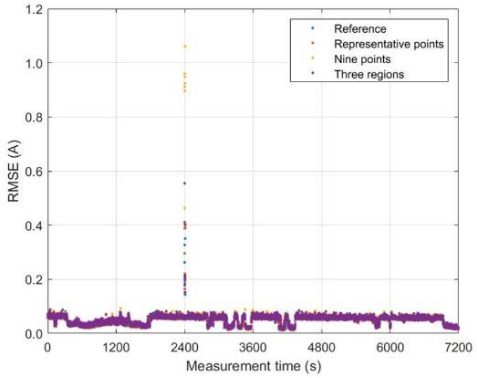

Figure 3: RMSE of the fitted single-diode model in terms of current to the measured *I-U* data preprocessed with the four approaches. 1 Hz *I-U* curve sampling frequency has been applied for two hours.

Table I. Median and IQR of RMSE values of the fitted single-diode model in terms of current to the measured two-hour *I-U* data preprocessed using the four approaches.

Approach	Median (A)	IQR (A)
Reference	0.0548	0.0279
Representative points	0.0532	0.0234
Nine points	0.0554	0.0231
Three regions	0.0551	0.0217

A more practical measure of the fit quality is its capability to repeat the directly measured outdoor conditions. Fig. 4 shows the irradiances provided by the four approaches as well as the measured irradiance values for the used two-hour *I-U* curve measurement data. The rapid irradiance changes are successfully captured by all the approaches. In line with [9] and [13] the irradiances obtained by the fits coincide, lying slightly above the measured values. The explanation for the latter fact lies in the procedure used to extract temperature from the fitted single-diode model and the use of Eq. (2). This is discussed in [9] in more depth.

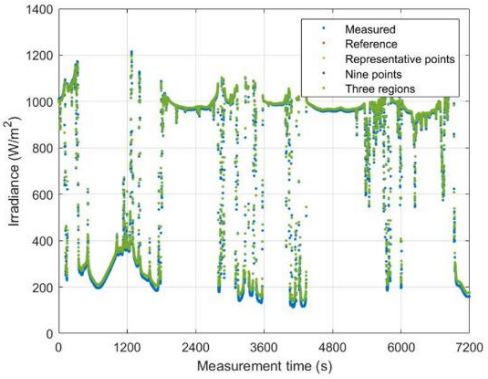

Figure 4: Irradiances obtained by fitting the single-diode model to the measurement data preprocessed with the four approaches jointly with the measured irradiance. 1 Hz *I-U* curve sampling frequency has been applied for two hours.

Temperatures provided by the four approaches are shown in Fig. 5 jointly with the measured values for the two-hour *I-U* curve measurement data. The corresponding temperature trends obtained by using moving average

smoothing are drawn in Fig. 6 to illustrate differences between the approaches more clearly. The temperatures closest to the measured temperature are provided by the three regions and reference approaches. The reference data has the major weighting in the open-circuit end of the measured curve providing naturally good temperature values, since the PV panel voltage is strongly dependent on the panel temperature. Although the three regions data are weighted equally around the main quantitative points of the curve, it forces the fit to follow the curvature of the *I-U* curve, leading to similar results.

In contrast, the temperatures obtained via the representative point approach deviate from the ones provided by the above approaches particularly for low irradiance values. The equal weighting of the measured curve leads to a reduced fit quality in the open-circuit end of the curve and an overestimation of the open-circuit voltage, thus lowering the fitted temperature values. On the other hand, the fit quality is improved for the other regions of the *I-U* curve, so this approach acts as a "trade-off". This approach is vulnerable also to the fact that the single-diode model performs worse at low irradiance levels.

Finally, the largest deviation from measured temperature is provided by the nine points approach. Moreover, the corresponding temperature trend curve exhibits sharp sawing. This is expected due to the exclusion of the detected MPP from the fitting points; the fit slightly surpasses the MPP, making the retrieval of the open-circuit end of the curve unstable.

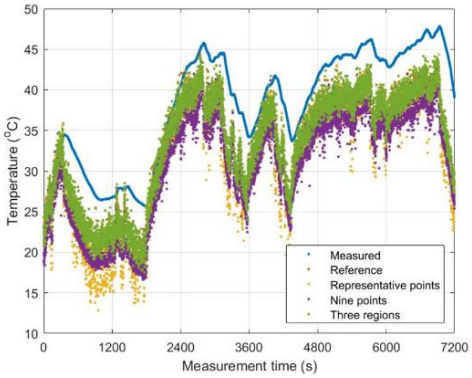

Figure 5: PV panel temperatures obtained by fitting the single-diode model to the measured *I-U* curves preprocessed with the four approaches jointly with the measured temperature. 1 Hz *I-U* curve sampling frequency has been applied for two hours.

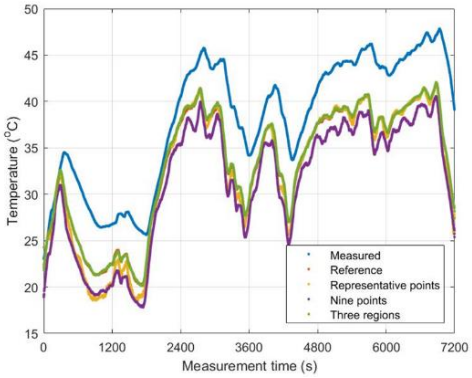

Figure 6: The temperature trends of Fig. 5.

Of the fitted single-diode model parameters, series resistance is the most important on the aging point of view. Fig. 7 shows the series resistances identified by the four approaches as a function of measurement time for the same two-hour *I-U* curve measurement data as already used in Figs. 3-6. The obtained series resistances seem to have quite stable values at high irradiances close to the known initial series resistance of the panel, but have been strongly underestimated in all the approaches at low irradiances. Therefore, we have analyzed the effect of irradiance on the obtained series resistance more closely. Further, there seems to be differences between the used preprocessing approaches. Using the same data, Figs. 8-11 provide the series resistance obtained by the four approaches as a function of the measured irradiance. It can be seen that the series resistance is downward as a function of irradiance in all the approaches. For a closer look Tables II-IV provide the median and IQR values for series resistances obtained by the four approaches for three separate one-hour *I-U* curve datasets: high (more than 800 W/m^2), medium (400-800 W/m^2) and low (less than 400 W/m^2) irradiance, respectively.

At high irradiance levels, the median R_s is approximately 0.7 Ω for all the approaches, with the reference approach providing the lowest median value. The smallest IQR is produced by the reference approach, which provides clearly most stable results at high irradiances as seen in Fig. 8 and Table II. A partial shading event is visible as downward pointing peaks in Fig. 7 around 2400 seconds and in Figs. 8-11 around 950 W/m^2.

At medium irradiance levels, the median R_s values are slightly below 0.7 Ω for all the approaches (Table III), with the representative points approach having the highest median value close to 0.7 Ω. This indicates that the representative points approach generally provides the most stable values at medium and high irradiances in line with Fig. 9. The IQR values are close to each other for all the approaches, with the reference approach having still the smallest value.

At low irradiance levels, the median R_s values are significantly lower, being around or below 0.6 Ω for all the approaches (Table IV), with a fairly large variation between the approaches. The IQR values are also very high for all the approaches. These results show that it is not possible to distinguish reliable series resistance values of PV modules under low irradiance condition at all, which is in line with findings in [1] and [13] and the known improper performance of the single-diode model at low irradiances. Perhaps the use of a better electrical model of the PV panel especially at low irradiances could solve the problem. On the other hand, practical analyzes could be limited to high irradiances to overcome this problem.

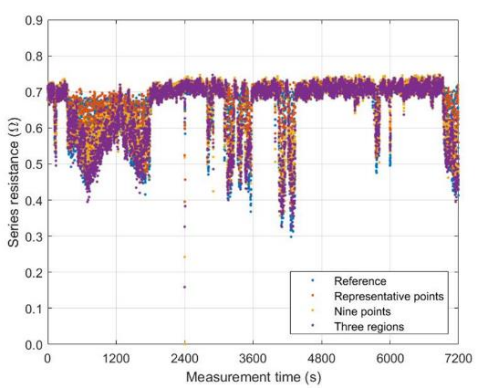

Figure 7: PV panel series resistance obtained by fitting the single-diode model to the measured *I-U* curves

preprocessed with the four approaches. 1 Hz *I-U* curve sampling frequency has been applied for two hours.

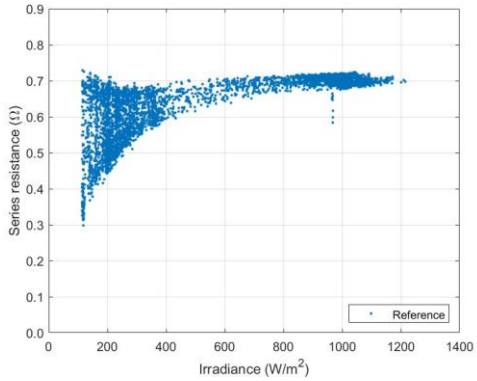

Figure 8: PV panel series resistance as a function of irradiance obtained by fitting the single-diode model to the measured *I-U* curves preprocessed with the reference approach.

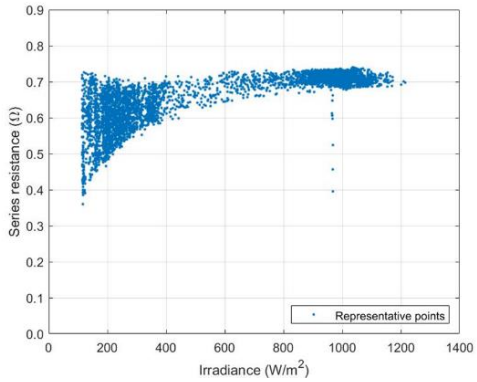

Figure 9: PV panel series resistance as a function of irradiance obtained by fitting the single-diode model to the measured *I-U* curves preprocessed with the representative points approach.

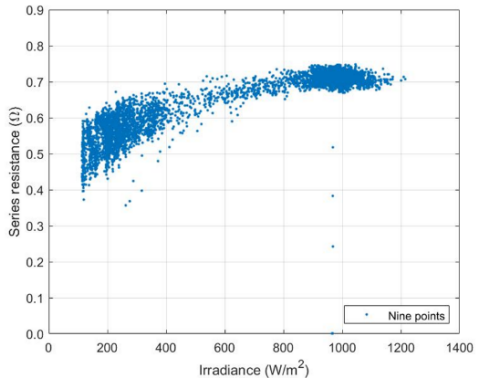

Figure 10: PV panel series resistance as a function of irradiance obtained by fitting the single-diode model to the measured *I-U* curves preprocessed with the nine points approach.

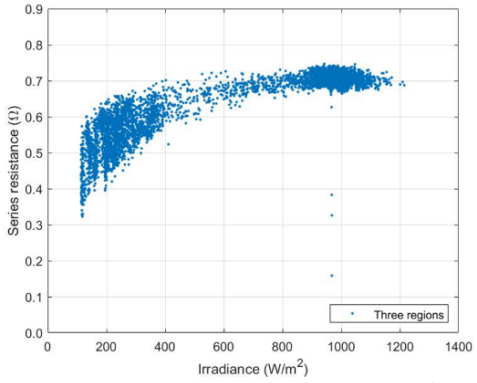

Figure 11: PV panel series resistance as a function of irradiance obtained by fitting the single-diode model to the measured *I-U* curves preprocessed with the three regions approach.

Table II: Median series resistance and the corresponding IQR value for one-hour high-irradiance *I-U* curve measurement data using the four approaches.

Approach	Median (Ω)	IQR (Ω)
Reference	0.7030	0.0120
Representative points	0.7092	0.0189
Nine points	0.7091	0.0200
Three regions	0.7058	0.0192

Table III: Median series resistance and the corresponding IQR value for one-hour medium-irradiance *I-U* curve measurement data using the four approaches.

Approach	Median (Ω)	IQR (Ω)
Reference	0.6909	0.0169
Representative points	0.6992	0.0259
Nine points	0.6874	0.0286
Three regions	0.6910	0.0277

Table IV: Median series resistance and the corresponding IQR value for one-hour low-irradiance *I-U* curve measurement data using the four approaches.

Approach	Median (Ω)	IQR (Ω)
Reference	0.5996	0.1170
Representative points	0.6130	0.0822
Nine points	0.5701	0.0684
Three regions	0.5634	0.0932

In conclusion, the identification of series resistance works well for high irradiance levels as expected. Further analyzes are needed to obtain reliable series resistance values at low irradiances as well as values for other aging and condition monitoring related parameters.

5 SUMMARY

This paper presented a detailed fitting procedure of the single-diode model to measured current-voltage characteristics. Four different measurement data preprocessing approaches were introduced to mitigate the problem of uneven weighting of datapoints caused by the *I-U* curve tracers. Their performance on returning the single-diode model parameter values were analyzed for obtaining more reliable diagnosis. All the approaches provided irradiance values close to the measured

irradiance. The resulting PV panel temperatures for all the approaches were also in line with the measured PV panel temperatures. Differences in series resistance values between different measurement point selection approaches are of particular interest for diagnosis of aging of PV panels. Measurements made at high irradiances appear to be a prerequisite for successful aging analysis.

References

[1] H. Kalliojärvi-Viljakainen, G. Spagnuolo, S. Valkealahti, Proceedings of 36th European Photovoltaic Solar Energy Conference and Exhibition, Marseille, France (2019) 1593.

[2] M. G. Villalva, J. R. Gazoli, E. R. Filho, IEEE Transactions on Power Electronics, Vol. 24 (2009) 1198.K.W. Boer, Solar Cells 16 (1996) 591.

[3] V. Leite, J. Batista, F. Chenlo, J. Afonso, International Conference on Renewable Energies and Power Quality (2012).

[4] J. Phang, D. Chan, Conference record of the IEEE Photovoltaic Specialists Conference (1985) 758.

[5] T. Zdanowicz, Proceedings 12th European Photovoltaic Solar Energy Conference (1994) 1311.

[6] A. Polman, W. Van Sark, W. Sinke, F. Saris, Solar Cells, Vol. 17(2-3) (1986) 241.

[7] N. Veissid, D. Bonnet, H. Richter, Solid-State Electronics, Vol. 38(11) (1995) 1937.

[8] A. Vega, V. Valiño, E. Conde, A. Ramos, P. Reina, Solar Energy, Vol. 190 (2019) 622.

[9] H. Kalliojärvi-Viljakainen, K. Lappalainen, S. Valkealahti, 47th IEEE Photovoltaic Specialists Conference (2020).

[10] G. Petrone, C. Ramos-Paja, G. Spagnuolo, John Wiley & Sons Ltd. (2017).

[11] D. Torres Lobera, S. Valkealahti, Proceedings of 27th European Photovoltaic Solar Energy Conference and Exhibition, Frankfurt, Germany (2012) 3905.

[12] G. Walker, Journal of Electrical & Electronics Engineering, Vol. 21(1) (2001) 49.

[13] K. Lappalainen, P. Manganiello, M. Piliougine, G. Spagnuolo, S. Valkealahti, IEEE Journal of Photovoltaics, Vol. 10(3) (2020) 852.